

PAPER • OPEN ACCESS

Numerical investigation on melting of Phase Change Material (PCM) dispersed with various nanoparticles inside a square enclosure

To cite this article: Tung Hao Kean *et al* 2019 *IOP Conf. Ser.: Mater. Sci. Eng.* **469** 012034

View the [article online](#) for updates and enhancements.



IOP | ebooksTM

Bringing you innovative digital publishing with leading voices to create your essential collection of books in STEM research.

Start exploring the collection - download the first chapter of every title for free.

Numerical investigation on melting of Phase Change Material (PCM) dispersed with various nanoparticles inside a square enclosure

Tung Hao Kean¹, Nor Azwadi Che Sidik¹, Jesbains Kaur²

¹Malaysia – Japan International Institute of Technology (MJIIT), University Teknologi Malaysia Kuala Lumpur, Jalan Sultan Yahya Petra (Jalan Semarak), 54100 Kuala Lumpur, Malaysia

²Research Centre for Nano-Materials and Energy Technology, School of Science and Technology, Sunway University, Bandar Sunway, 47500 Subang Jaya Selangor, Malaysia

*Corresponding author: azwadi@utm.my

Abstract. A numerical investigation on melting of Phase Change Material (PCM) after dispersed with various types of nanoparticles is presented in this study. Nanoparticles with high thermal conductivity properties could be a good additive to enhance the thermal performance of PCM in latent heat thermal energy storage. This paper focus on the melting rate of paraffin wax as PCM dispersed with three types of nanoparticles: Alumina (Al_2O_3), Copper oxide (CuO) and Zinc Oxide (ZnO) in a 25mm × 25mm square enclosure. The effect of heating side of the wall and the concentration of nanoparticles dispersed in PCM were investigated. ANSYS Workbench 17.0 that included mesh generation tools and FLUENT software was used to run the simulation. Enthalpy porosity method was applied in this numerical study. Results shown that heat transfer rate was improved by adding low volume fraction of nanoparticles. Heating from the side wall of the enclosure has better melting rate than heating from below.

1. Introduction

Since past decades, thermal energy storage (TES) incorporating with phase change material (PCM) were getting great attention due to the ideal properties of PCM in storing and releasing thermal energy during the process of melting and freezing. Abundance of energy can be stored or released at a nearly constant temperature during the phase change process [1-3]. Nevertheless, the relatively low thermal conductivity in the nature of PCM is a great drawback that affects the performance of TES. Apparently past researchers has suggested two main approaches for enhancing the thermal conductivity of a PCM The first approach is refinement in the design of the geometry of the container or installation of fixed materials such as metal fins and porous materials which are highly thermal conductive inside the enclosure. The other approach is based on dispersion of highly conductive nanoparticles such as metal oxide with PCM to increase its overall thermal conductivity[4-6].

There have been also many previous studies on the phase change of PCMs in different enclosures. The pioneer research was conducted by Khodadadi and Hosseinizadeh [7] in year 2007 that performed the investigation on heat transfer enhancement of PCM thought dispersion of nanoparticles . Inspired by the report of Mesuda [8], Khodadadi and Hosseinizadeh numerically study the potential of using nanoparticle-enhanced phase change material (NEPCM) in TES applications. By using copper nanoparticles and water as PCM, they studied the freezing of the NEPCM in a differentially-heated



square enclosure that started with steady state natural convection. They discovered that for a fixed Grashof number, the solidification time was decreased as the volume fraction of nanoparticles increased. The increment in freezing rate indicating the enhancement of thermal conductivity of the NEPCM in comparison to that of the base PCM. Besides, less energy per unit mass is needed for the freezing of the NEPCM.

Arasu and Mujumdar [9] performed a numerical simulation on the melting of PCM (paraffin wax) dispersed with various volume fractions of nanoparticles (Al_2O_3) inside a square cavity where the wall was heated from horizontal bottom or left vertical side. The results shown that adding 2 wt.% Al_2O_3 nanoparticles can enhance melting rate. However, dispersing volume fraction more than 2 wt.% caused the natural convection weaken due to increment in viscosity and slower the melting rate of NEPCM. They also discovered that the melting rate and energy stored are higher for vertical wall heating than horizontal bottom wall heating in a square enclosure due to domination of natural convection. Sebt et al.[10] also carried out a numerical study on melting process of a PCM in a square cavity in order to investigate the heat transfer improvement of base PCM by adding Cu nanoparticles. They concluded that the heat transfer rate of NEPCM increased as the melting time reduced when the concentration of nanoparticles dispersed in PCM increased. Two years later, a numerical simulation on melting of NEPCM in a square enclosure with two heat source-sink was carried out by Aziz and Abdolrahman [11]. They studied four different orientations of the source and sink, thus the results indicated that the liquid fraction of NEPCM is the highest at the final stage of melting when the sources and sinks are alternately placed on two vertical sidewalls. They also found that 2% of nanoparticles volumetric concentration given the highest melting rate in all case of the study.

In this present work, a numerical investigation on melting of PCM to study the heat transfer rate enhanced by dispersing nanoparticles was carried out. PCM applied in the study was paraffin wax whereas nanoparticles were Alumina(Al_2O_3), Copper oxide (CuO) and Zinc Oxide (ZnO). Various volume fractions (0 %, 2 % & 5 %) of nanoparticles dispersed with PCM was examined and the position of the heat transfer surface in a square enclosure (25 mm×25 mm) was reported.

2. Physical Model

The geometry applied was shown in Figure 1. It is a square enclosure with a dimension of 25 mm (L) ×25 mm (W). The cavity filled with pure PCM or PCM dispersed with numerous type of nanoparticles with different volume fraction. There are two case study where one of the hot wall are located at the left vertical wall and the other at the horizontal bottom wall. The temperature of the hot wall is at constant temperature of 330 K and the opposite wall, also known as cold wall is at a constant temperature of 300 K. The remaining two walls are adiabatic and the initial temperature of the PCM is 300K. Note that the following assumptions have been made in present work:

- The flow of NEPCM in liquid state is considered as an incompressible, unsteady, laminar and Newtonian.
- The viscous dissipation, thermal radiation, 3D convection and volumetric expansion are negligible.
- The thermal physical properties of PCM and NEPCM are temperature dependent.
- Heat transfer is both conduction and convection controlled.
- The PCM or nanoparticles are assumed as continuous media and in state of thermodynamic equilibrium.
- There is no-slip boundary condition is applied between PCM and nanoparticles.

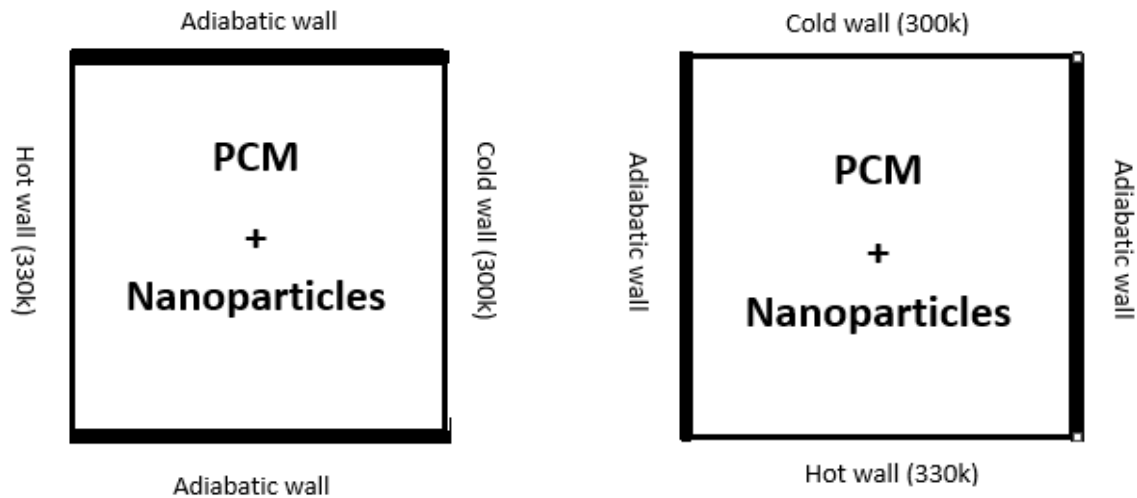


Figure 1 a). Square cavity (25 mm×25 mm) heating from left vertical side

Figure 1 b). Square cavity (25 mm×25 mm) heating from bottom

3. Governing Equation

Enthalpy porosity method is used in present simulation on melting of a NEPCM in a square enclosure. The enthalpy porosity method can figure out the liquid fraction in each cell in the computational domain at any iteration based on enthalpy balance. During the phase change process, the value of liquid fraction changes between 0 and 1 where the values of 0 represent solid state and 1 represent liquid state respectively. Also, values lie between 0 and 1 are serve as mushy state. The governing conservation equations are as follows [12]:

Continuity equation:

$$\frac{\partial \rho}{\partial t} + \nabla \cdot (\rho \vec{U}) = 0 \quad (1)$$

Momentum equation:

$$\frac{\partial}{\partial t} (\rho \vec{U}) + \nabla \cdot (\rho \vec{U} \vec{U}) = -\nabla P + \rho \vec{g} + \nabla \vec{\tau} + \vec{F} \quad (2)$$

where P represents the static pressure, $\vec{\tau}$ denotes the stress tensor, $\rho \vec{g}$ is the gravitational body force and \vec{F} is the external body force.

Energy equation:

$$\frac{\partial (\rho H)}{\partial t} + \nabla \cdot (\rho \vec{U} H) = \nabla \cdot (K \nabla T) + S \quad (3)$$

where H is the enthalpy of NEPCM, T denotes the temperature, ρ represent density, K is thermal conductivity of NEPCM, \vec{U} stands for velocity and S is the source volumetric heat source term which is set for zero in present work. The total enthalpy H , of the PCM is considered as the sum of the sensible enthalpy, h and the latent heat, ΔH :

$$H = h + \Delta H \quad (4)$$

where

$$h = h_{ref} + \int_{T_{ref}}^T C_p dT \quad (5)$$

Here, T_{ref} and h_{ref} are the reference temperature and reference enthalpy respectively. C_p represents the specific heat at constant pressure. Also, the latent heat of the PCM is given by:

$$\nabla H = \beta L \quad (6)$$

where β is the liquid fraction and is defined as:

$$\beta = \begin{cases} 0 & T < T_{solidus} \\ \frac{T - T_{solidus}}{T_{liquidus} - T_{solidus}} & \text{if } T_{solidus} < T < T_{liquidus} \\ 1 & T > T_{liquidus} \end{cases} \quad (7)$$

There is a necessitate to have iteration between the energy Eq (3) and liquid fraction Eq (6) to solve temperature. In enthalpy porosity method, the mushy region (partially solidified region) is treated as a porous medium. The porosity in each cell is set equal to the liquid fraction in that cell. In fully solidified regions, porosity is set equal to zero, which excluded the velocities in these regions.

The boundary condition in present study is prescribed as follow:

- Hot Wall: $T = T_{max}$
- Cold Wall: $T = T_{min}$
- Adiabatic Wall: $K_{np\text{pcm}} \Delta T = 0$
- Initial Condition: $T_i = T_{min}$

4. Thermal Physical Properties

The thermal physical properties of PCM and nanoparticles are listed in Table 1. The difference in the solidus and liquidus temperatures denotes the phase transition from solid to liquid state in the melting of PCM. The density, latent heat and specific heat capacity of the NEPCM are defined as follows [13]:

$$\rho_{np\text{pcm}} = \phi \rho_{np} + (1 - \phi) \rho_{pcm} \quad (8)$$

where ρ_{np} and ρ_{pcm} are the density of nanoparticles and density of PCM respectively, while ϕ is the volumetric concentration of nanoparticles.

$$L_{np\text{pcm}} = \frac{(1 - \phi)(\rho L)_{pcm}}{\rho_{np\text{pcm}}} \quad (9)$$

$$Cp_{np\text{pcm}} = \frac{\phi(\rho Cp)_{np} + (1 - \phi)(\rho Cp)_{pcm}}{\rho_{np\text{pcm}}} \quad (10)$$

where Cp_{np} and Cp_{pcm} are the specific heats of nanoparticles and PCM respectively. The dynamic viscosity is estimated by:

$$\mu_{np\text{pcm}} = \lambda_1 e^{(\lambda_2 \phi)} \quad (11)$$

The effective thermal conductivity is calculated from the correlation proposed by Vajjha et al. [14]. In the model, they combine the static part of Maxwell's theory and the dynamic part of the Brownian motion of nanoparticles which defined as:

$$K_{np\text{pcm}} = \frac{K_{np} + 2K_{pcm} - 2(K_{pcm} - K_{np})\phi}{K_{np} + 2K_{pcm} + 2(K_{pcm} - K_{np})\phi} K_{pcm} + 5 \times 10^4 \beta_k \zeta \phi_{pcm} Cp_{pcm} \sqrt{\frac{BT}{\rho_{np} d_{np}}} f(T, \phi) \quad (12)$$

where B is the Boltzmann constant, $1.381 \times 10^{-23} \text{ J/K}$ and

$$\beta_k = \beta_1(100\phi)^{\beta_2} \quad (13)$$

$$f(T, \phi) = \left(2.8217 \times 10^{-2} \phi + 3.917 \times 10^{-3}\right) \frac{T}{T_{ref}} + \left(-0.669 \times 10^{-2} \phi - 3.91123 \times 10^{-3}\right) \quad (14)$$

where T_{ref} is the reference temperature which is equal to 273 K. The correction factor, ζ in the Brownian motion term value is defined as the same for liquid fraction, β in Eq. (7) since there are no Brownian motion in the solid state.

Table 1. Properties of PCM, nanoparticles and operating parameters [15-17]

	Paraffin Wax	Al ₂ O ₃	CuO	ZnO
Density (kg/m ³)	750	3600	6510	5606
	$0.001(T - 319.15) + 1$			
Specific heat (J/kgK)	2890	765	540	514
Thermal conductivity (W/mK)	0.21 if $T < T_{solidus}$ 0.12 if $T > T_{liquidus}$	36	18	23.4
Dynamic Viscosity (Ns/m ²)	$0.001 \exp\left(-4.25 + \frac{1700}{T}\right)$	-	-	-
Latent heat (J/kg)	173400	-	-	-
Solidus temperature (K)	319	-	-	-
Liquidus temperature (K)	321	-	-	-
d_{np} (nm)	-	59	29	50
λ_1	-	0.983	0.9197	0.904
λ_2	-	12.958	22.8539	14.8
β_1	-	8.4407	9.881	8.4407
β_2	-	-1.07304	-0.9446	-1.07304

5. Computational Methodology & Grid Independence Test

In present numerical study, the integrated simulation system ANSYS Workbench 17.0 is used. The governing equations that related to the boundary and initial conditions are solved by the FLUENT software based on the finite volume method. The SIMPLE algorithm is applied for solving pressure–velocity coupling and the PRESTO scheme is used for the pressure correction equation. FIRST ORDER UPWIND differencing scheme is adopted on the momentum and energy equations. For all iterations, the time step for integrating the temporal derivatives was set to 0.01s. whereas for every time step, the maximum number of iterations is adjusted to 10 which is adequate with the convergence limit of 10^{-3} in the continuity and momentum equations; 10^{-6} in the energy equation. Also, for the under-relaxation factors for x-components and y-components, momentum equations, pressure correction equation, energy equation, and liquid fraction are fixed to 0.5, 0.3, 1 and 1 respectively.

A mesh test is conducted in order to check the grid independence and refine the obtained results. A graph of liquid fraction over flow time is plotted as shown Figure 2 with 0 % of Al₂O₃. Grid sizes of 80×80 , 100×100 and 110×110 are simulated. According to the Figure 2, there is negligibly small

difference between the results of the 100×100 and 110×110 grid sizes. Hence, the grid with 100×100 cells is considered and selected for all the simulations and calculations in present work.

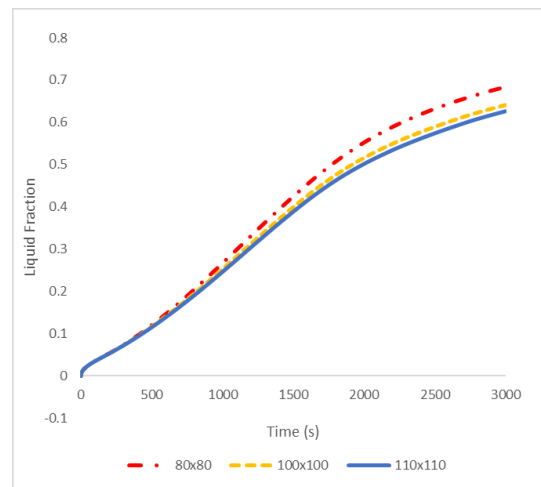


Figure 2. Effect of Grid Size on Melting of Pure PCM

6. Model Validation

Similar simulation was reported by Arasu and Mujumdar [9] and Ebrahimi [11] on melting of NEPCM in a square enclosure using paraffin wax as PCM and mixing with 2 wt.% of Al_2O_3 nanoparticles. The results of liquid–solid interface at 1000 s and 3000 s is compared and shown in Figure 3. A reasonably good agreement is obtained.

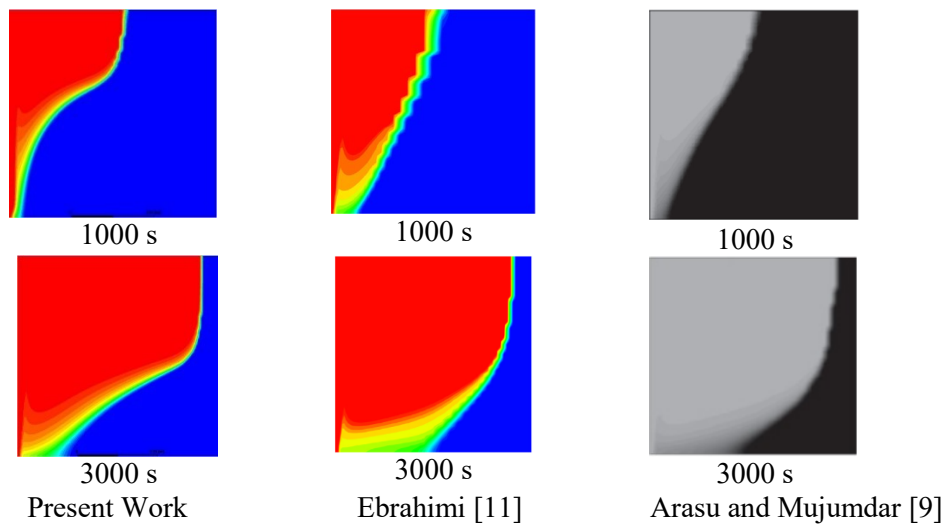


Figure 3. Comparison on Melting of Paraffin Wax + 2 % Al_2O_3 Nanoparticles

7. Results & Discussion

By using the numerical model mentioned above, the melting of pure PCM and NEPCM in a square cavity are carried out by heating from the horizontal bottom side followed by left vertical side. The simulation condition is displayed in Table 2 whereas the results are presented and discussed below.

Table 2. Test condition.

PCM/NEPCM	Concentration	Time
Paraffin Wax	-	1000 s, 3000 s
Paraffin Wax + Al ₂ O ₃	2 %, 5 %	1000 s, 3000 s
Paraffin Wax + CuO	2 %, 5 %	1000 s, 3000 s
Paraffin Wax + ZnO	2 %, 5 %	1000 s, 3000 s

7.1 Thermal-Physical Properties

Figure 4 and 5 indicates the thermal-physical properties of pure PCM and NEPCM. By applying Eq (11) and Eq (12), the change in thermal conductivity and dynamic viscosity of paraffin wax dispersed with 0 %, 2 % and 5 % of metal oxides (Al₂O₃, CuO, ZnO) are plotted as the function of temperature and volume fraction. Based on Figure 4, it can be observed that the thermal conductivity of the NEPCM is higher than pure PCM. At temperature range of 300 K to 320 K, the thermal conductivity is maintained at constant as the PCM/NEPCM are probably still in solid state. On the other hand, between temperatures 320 K to 360 K, the thermal conductivity of PCM increases with the rising temperature and volumetric concentration of dispersed nanoparticles. Additional 5 % CuO nanoparticles dispersed into the paraffin wax gives the highest enhancement effect in thermal conductivity compared with other test conditions.

From Figure 5, the dynamic viscosity of PCM/NEPCM decreases as the temperature increases. Besides, there is an augmentation in dynamic viscosity as the volume fraction of nanoparticles added to the pure PCM become higher. The increment of viscosity is much more significant at low temperature (300 K) compared to that at high temperature (360 K) due to the high Brownian motion of nanoparticles at high temperature. The enhancement in dynamic viscosity plays a key role in the melting proses as the natural convection is dominating the heat transfer mechanism. In addition, dispersion of 5 % CuO nanoparticles into paraffin wax resulting the greatest augmentation in dynamic viscosity. Overall, the variations in the thermal-physical properties of PCM/NEPCM are reasonable and are in well agreement with the experimental results reported by Ho and Gao [18].

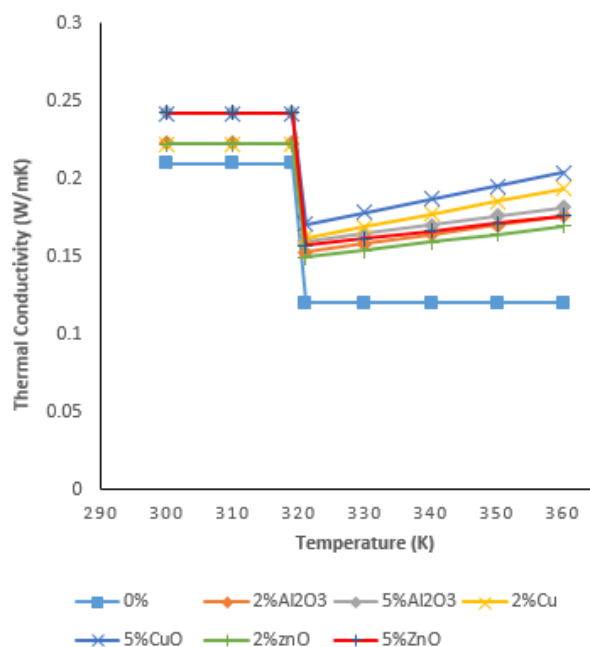


Figure 4. Variations in thermal conductivity of PCM/NEPCM with different volume fractions of nanoparticles and temperature.

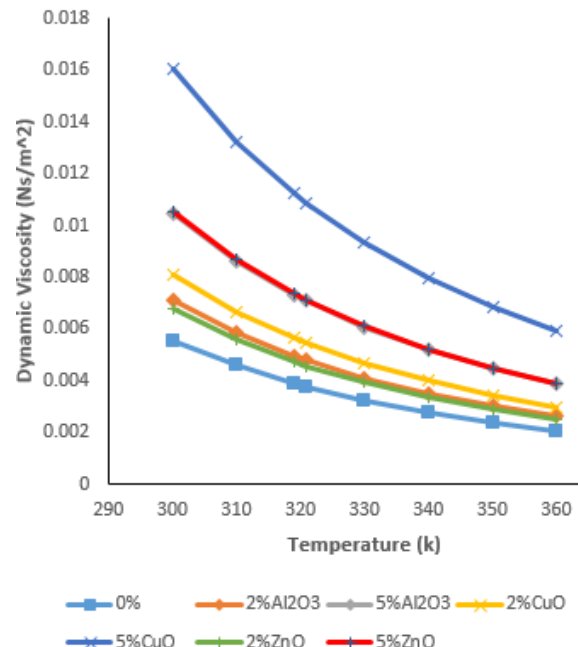


Figure 5. Variations in dynamic viscosity of PCM/NEPCM with different volume fractions of nanoparticles and temperature.

7.2 Evolution of Melting Rate

The effect of mixing nanoparticles with PCM on its melting rate is examined and the result is plotted in Figure 6. The melting rate is indicated by the liquid fraction contained at certain time being. According to Figure 6, it is clear that the melting rate of PCM can be improved by adding 2 % of nanoparticles but only at low concentration. On the other hand, PCM melt slower when 5 % of metal oxide is added. This trend justifies that improvement in thermal conductivity can enhance the melting rate but high dynamic viscosity will degrade the heat transfer rate. In first 400 s, there is no significant difference in melting speed of all PCM/NEPCM as the conduction is dominant at the heat transfer rate at initial stage. Effect of dynamic viscosity becomes greater when dominant mechanism become convection during melting and may overweight the improvement in thermal conductivity. Thus, the heat transfer performance enhancement of NEPCM is only applicable at low volume fraction. In present study, greatest enhancement in melting rate is obtained by dispersion of 2 % Al_2O_3 nanoparticles in paraffin wax. Table 3 displays the liquid fraction of PCM/NEPCM at melting period of 3000 s. On the other hand, adding 5 % CuO nanoparticles results in significant degradation in heat transfer.

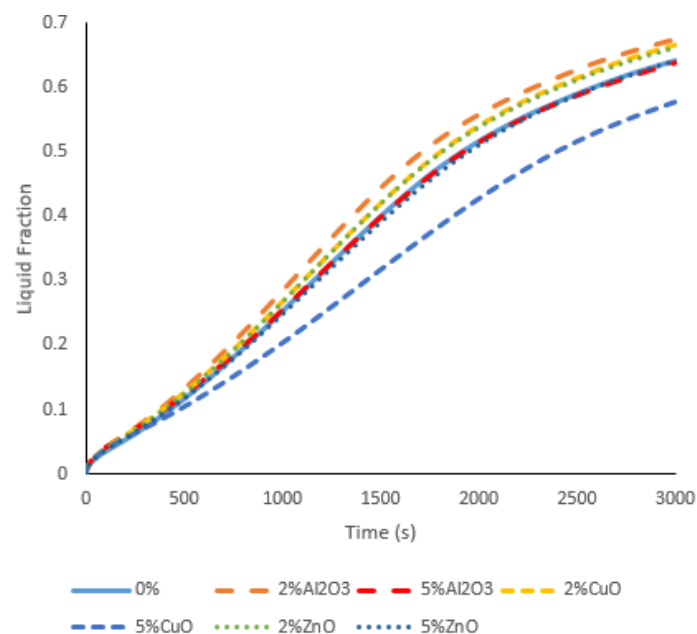


Figure 6. Liquid Fraction of PCM/NEPCM.

Table 3. Liquid Fraction at time 3000s.

PCM/NEPCM	Concentration	Liquid Fraction
Paraffin Wax	-	0.6412
Paraffin Wax + Al_2O_3	2 %	0.6742
	5 %	0.6380
Paraffin Wax + CuO	2 %	0.6654
	5 %	0.5771
Paraffin Wax + ZnO	2 %	0.6613
	5 %	0.6408

7.3 Effect of Heating Surface Orientation

Melting of paraffin wax with 2 % of Al_2O_3 heating form side and below are shown in Figure 7 and Figure 8. For both cases, the liquid–solid interface is flat at the initial stage of melting process as conduction is the initial heat transfer mechanism and the buoyancy forces cannot overweight the resistance inflicted by the viscose forces. After that, convection takes place and the liquid–solid interface slowly becomes more and more distorted as the fluid motion become stronger. The liquid–solid interface

moves faster at zone where the heated fluid flow is upward but slower at the zone where the fluid flow is downward. Nevertheless, for vertical side heating, development of liquid phase causes the hot liquid to ascend whereas the cold liquid PCM to descend. As the time passed, the temperature of liquid at the upper zone is higher than that in lower zone. Thus, the melting process in the upper zone is more advanced. As a results, there is more liquid interface near the upper zone of the square enclosure.

According to Figure 9, the overall melting rate of paraffin wax heated from the vertical side is higher than that heated from below at 3000 s. However, during the melting period 1000 s to 1500 s, the melting speed of paraffin wax heated from below is faster compared with heated from the side. This melting trend is probably due to the formation of multi-cellular flow patterns when heating from below. In addition, the enhancement effect in melting rate is highest when 2 % of Al_2O_3 dispersed into paraffin wax for both heating surface.

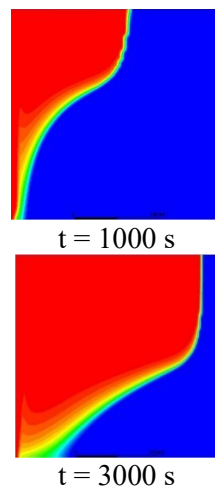


Figure 7. Melting of PCM heating from left vertical side.

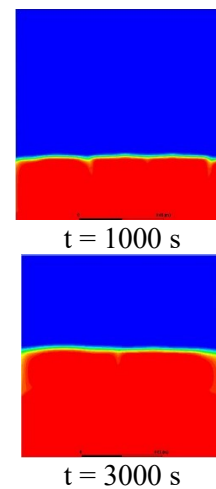


Figure 8. Melting of PCM heating from bottom.

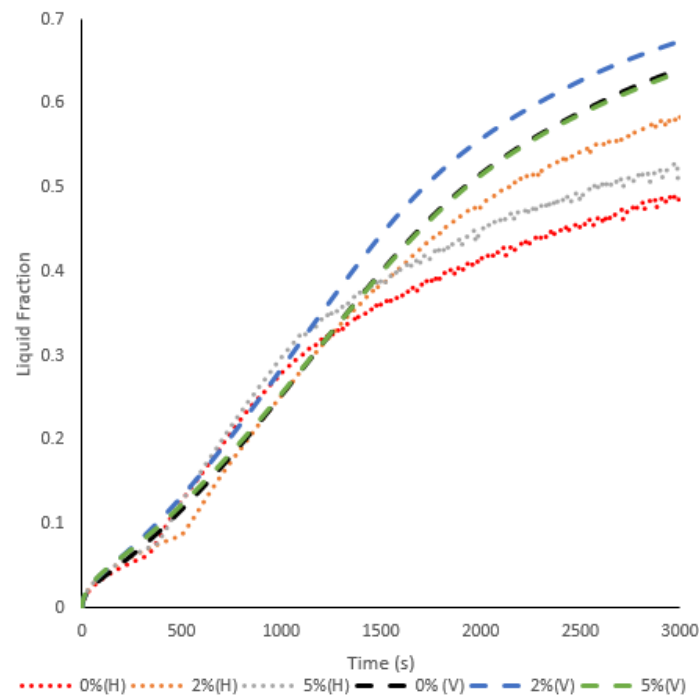


Figure 9. Liquid Fraction of PCM/NEPCM Heated from Vertical side (V) and Bottom (H).

8. Conclusion

In this paper, a numerical study on the melting of PCM dispersed with various types and volume fractions of nanoparticles in square cavity is carried out using enthalpy porosity method. From the investigation, it can be concluded that addition of nanoparticles can augment the effective thermal conductivity but also increase the dynamic viscosity of the composite. Therefore, the heat transfer performance of PCM only can be enhanced by low volumetric concentration of nanoparticles. Too much nanoparticles loading may cause high viscosity and degrade the heat transfer rate. Besides, the best improvement in melting rate in present work was achieved by the combination of paraffin wax and 2 % Al_2O_3 nanoparticles which is around 5.15 %. In contrast, combination of paraffin wax with 5 % CuO nanoparticles slow down the melting speed of PCM by 9.98 %. Last but not least, the melting rate for vertical side heating was higher than horizontal bottom heating in a square enclosure. For the future works, the numerical simulation on solidification process of PCM and NEPCM will be done to obtain a phase change energy cycle diagram since more energy can be conserved as TES can function at high efficiency when incorporating with NEPCM.

Acknowledgement

Authors wish to thank Universiti Teknologi Malaysia. The paper was supported by Takasago grant (Vote no.: R.K130000.7343.4B314)

10. References

- [1] Farid M M, Khudhair A M, Razack S A K and Al-Hallaj S 2004 A review on phase change energy storage: materials and applications *Energy conversion and management* **45** 1597-615.
- [2] Cabeza L F, Castell A, Barreneche C, De Gracia A and Fernández A 2011 Materials used as PCM in thermal energy storage in buildings: a review *Renewable and Sustainable Energy Reviews* **15** 1675-95.
- [3] Zalba B, Marin J M, Cabeza L F and Mehling H 2003 Review on thermal energy storage with phase change: materials, heat transfer analysis and applications *Applied thermal engineering* **23** 251-83.
- [4] Ebadi S, Tasnim S H, Aliabadi A A and Mahmud S 2018 Melting of nano-PCM inside a cylindrical thermal energy storage system: Numerical study with experimental verification *Energy Conversion and Management* **166** 241-59.
- [5] Fan L and Khodadadi J M 2011 Thermal conductivity enhancement of phase change materials for thermal energy storage: a review *Renewable and Sustainable Energy Reviews* **15** 24-46.
- [6] Ibrahim N I, Al-Sulaiman F A, Rahman S, Yilbas B S and Sahin A Z 2017 Heat transfer enhancement of phase change materials for thermal energy storage applications: a critical review *Renewable and Sustainable Energy Reviews* **74** 26-50.
- [7] Khodadadi J and Hosseinizadeh S 2007 Nanoparticle-enhanced phase change materials (NEPCM) with great potential for improved thermal energy storage *International communications in heat and mass transfer* **34** 534-43.
- [8] Masuda H, Ebata A and Teramae K 1993 Alteration of thermal conductivity and viscosity of liquid by dispersing ultra-fine particles. Dispersion of Al_2O_3 , SiO_2 and TiO_2 ultra-fine particles.
- [9] Arasu A V and Mujumdar A S 2012 Numerical study on melting of paraffin wax with Al_2O_3 in a square enclosure *International Communications in Heat and Mass Transfer* **39** 8-16.
- [10] Sebti S S, Mastiani M, Mirzaei H, Dadvand A, Kashani S and Hosseini S A 2013 Numerical study of the melting of nano-enhanced phase change material in a square cavity *Journal of Zhejiang University SCIENCE A* **14** 307-16.
- [11] Ebrahimi A and Dadvand A 2015 Simulation of melting of a nano-enhanced phase change material (NePCM) in a square cavity with two heat source–sink pairs *Alexandria Engineering Journal* **54** 1003-17.
- [12] Retrived from: <http://www.fluent.com>. Available from: <http://www.fluent.com>.
- [13] Chow L, Zhong J and Beam J, editors. Thermal conductivity enhancement for phase change storage media. 24th Thermophysics Conference; 1996.

- [14] Vajjha R S, Das D K and Namburu P K 2010 Numerical study of fluid dynamic and heat transfer performance of Al₂O₃ and CuO nanofluids in the flat tubes of a radiator *International Journal of Heat and fluid flow* **31** 613-21.
- [15] Sasmito A P, Kurnia J C and Mujumdar A S 2011 Numerical evaluation of laminar heat transfer enhancement in nanofluid flow in coiled square tubes *Nanoscale research letters* **6** 376.
- [16] Kandasamy R, Wang X-Q and Mujumdar A S 2008 Transient cooling of electronics using phase change material (PCM)-based heat sinks *Applied thermal engineering* **28** 1047-57.
- [17] Alawi O A, Sidik N A C, Xian H W, Kean T H and Kazi S 2018 Thermal conductivity and viscosity models of metallic oxides nanofluids *International Journal of Heat and Mass Transfer* **116** 1314-25.
- [18] Ho C J and Gao J 2009 Preparation and thermophysical properties of nanoparticle-in-paraffin emulsion as phase change material *International Communications in Heat and Mass Transfer* **36** 467-70.